ELSEVIER

Journal of Alloys and Compounds 408–412 (2006) 1324–1328

Journal of ALLOYS AND COMPOUNDS

www.elsevier.com/locate/jallcom

Crystal structure and magnetic state of U_2XSi_3 (X = Fe, Pt)

T. Yamamura *, D.X. Li, K. Yubuta, Y. Shiokawa

Institute for Materials Research, Tohoku University, Sendai, Miyagi 980-8577, Japan

Available online 18 July 2005

Abstract

Atomic arrangement in U_2XSi_3 with X = Pt and Fe was investigated by electron diffraction and X-ray powder diffraction and discussed in conjunction with the results of magnetic susceptibility, magnetization, specific heat electrical resistivity measurements. U_2PtSi_3 crystallizes in the simple AlB_2-type structure, where Pt and Si atoms are located at B sites disorderly and shows spin glass behavior at low temperature. Contrarily, the electron diffraction pattern for U_2FeSi_3 reveals a superstructure doubling the lattice parameter as that observed for U_2RuSi_3, suggesting absence of the random structure. In this structurally ordered compound U_2FeSi_3, no spin glass behavior is detected.

Keywords: U_2FeSi_3; U_2PtSi_3; Electron diffraction; Atomic arrangement; Spin glass; Specific heat

1. Introduction

The ternary intermetallic compounds U_2XY_3 (X: transition metal, Y: typical element), which crystallize in disordered derivatives of the hexagonal AlB_2-type structure, have become a subject of intensive study because of the diversity of their magnetic properties. The compounds U_2XSi_3 exhibit spin glass behavior for X = Pt [1–3], Pd [3,4], Au [3,5], ferromagnetic cluster glass behavior for X = Ir [6], Rh [7] and paramagnetic ground state for X = Fe [7–9], Ru [7], Os [7]. The first work on the analysis of atomic arrangement in U_2RuSi_3, U_2PdSi_3 and U_2RhSi_3 was reported by Chevalier et al. in conjunction with their magnetic properties [7]. However, nothing was known about the atomic arrangement in U_2XSi_3 with X = Fe, Ir, Pt, Au, which show different magnetic properties at low temperatures, characterized as spin glass (X = Pt, Au), cluster glass (X = Ir) and paramagnet (X = Fe). Since it is generally accepted that randomness and frustration are two necessary conditions to form a spin glass state, investigation of the crystal structure and atomic distribution in these compounds is required for understanding their different magnetic properties.

Recently, there is an interesting discussion on this topic related to the series of the U_2XGa_3 compounds. Among the U_2XGa_3 compounds with X = Ru, Rh, Ir, Pd, Pt and Au, which crystallize in the orthorhombic $CeCu_2$-type structure (space group *Imma*) [10], three of them (X = Ru, Rh, Ir) show ferromagnetic properties with the Curie temperature of 73, 60 and 72 K [10], respectively, and other two compounds (X = Pd, Pt) are antiferromagnets with the Néel temperature of 33 and 30 K [10,11], respectively. Our magnetic and specific heat measurements revealed a spin glass state in the U_2AuGa_3 compound [12] in spite of a lack of geometrical frustration in the $CeCu_2$-type crystal structure, and thus, the occurrence of frustrated single-ion magnetic moment is not expected [11]. Instead, it seems that the statistical distribution of Au and Ga atoms in the crystal lattice could introduce the formation of magnetic clusters with randomly distributed exchange interactions between them, leading to a frustration and to a spin glass state. On the other hand, the U_2CuGa_3 compound is a special case in this series of compounds because it crystallizes in the AlB_2-type structure [13–15] and also exhibits spin glass behavior [13,16,17]. The neutron diffraction study by Tran et al. suggested that U_2CuGa_3 possesses the Lu_2CoGa_3-type structure (an ordered superstructure of AlB_2-type) with perfectly ordered arrangement of all atoms in the lattice [16], whereas our electron diffraction measurements for our U_2CuGa_3 sample indicate the AlB_2-type

* Corresponding author. Tel.: +81 22 215 2120; fax: +81 22 215 2121.
E-mail address: yamamura@imr.tohoku.ac.jp (T. Yamamura).

0925-8388/$ – see front matter © 2005 Elsevier B.V. All rights reserved.
doi:10.1016/j.jallcom.2005.04.184

structure with statistically distribution of Cu and Ga atoms on 2*d* sites.

In this study, atomic arrangements in U_2FeSi_3 and U_2PtSi_3 were investigated by electron diffraction and X-ray diffraction (XRD) measurements. Magnetic properties of these compounds were also studied and discussed in conjunction with their structure characteristics.

2. Experimental

Polycrystalline samples of U_2FeSi_3 and U_2PtSi_3 were synthesized by melting the stoichiometric amounts of constituent elements using an arc furnace with argon atmosphere. The purities of the starting materials are 5N for Fe, 4N for Pt, 6N for Si and 3N for U. Weight loss in the melting process is smaller than 0.2 wt%. Samples were then annealed at 800 °C for 10 days. X-ray powder diffraction was performed at room temperature with Cu Kα radiation and the obtained patterns were analyzed by a Rietveld analysis using RIETAN-2000 [18]. Electron diffraction measurements were carried out by using a JEOL JEM-2000FXII transmission electron microscope.

The temperature dependence of dc susceptibility $\chi(T) = M(T)/H$, the field dependence of magnetization $M(H)$ and magnetic relaxation $M(t)$ measurements were carried out in a SQUID magnetometer ($H = 0$–10 kOe). The adiabatic heat-pulse method was employed for specific heat measurements over the temperature range from 1.8 to 40 K. Electrical resistivity measurement was performed between 0.5 and 295 K using a standard four-terminal dc method.

3. Results and discussion

3.1. X-ray and electron diffraction study

The electron diffraction patterns of U_2PtSi_3 obtained along [0 0 1] and [1 0 0] axes are shown in Fig. 1(upper). It is clear that these electron diffraction patterns correspond to the hexagonal AlB_2-type structure (see the inset of Fig. 2(a)) and exclude existence of any superstructure, similar to that observed for U_2PdSi_3 [7]. Also, the X-ray diffraction peaks for U_2PtSi_3 shown in Fig. 2(a) can be well indexed by the hexagonal AlB_2-type structure model (space group *P*6/*mmm*) with the lattice parameters of $a =$

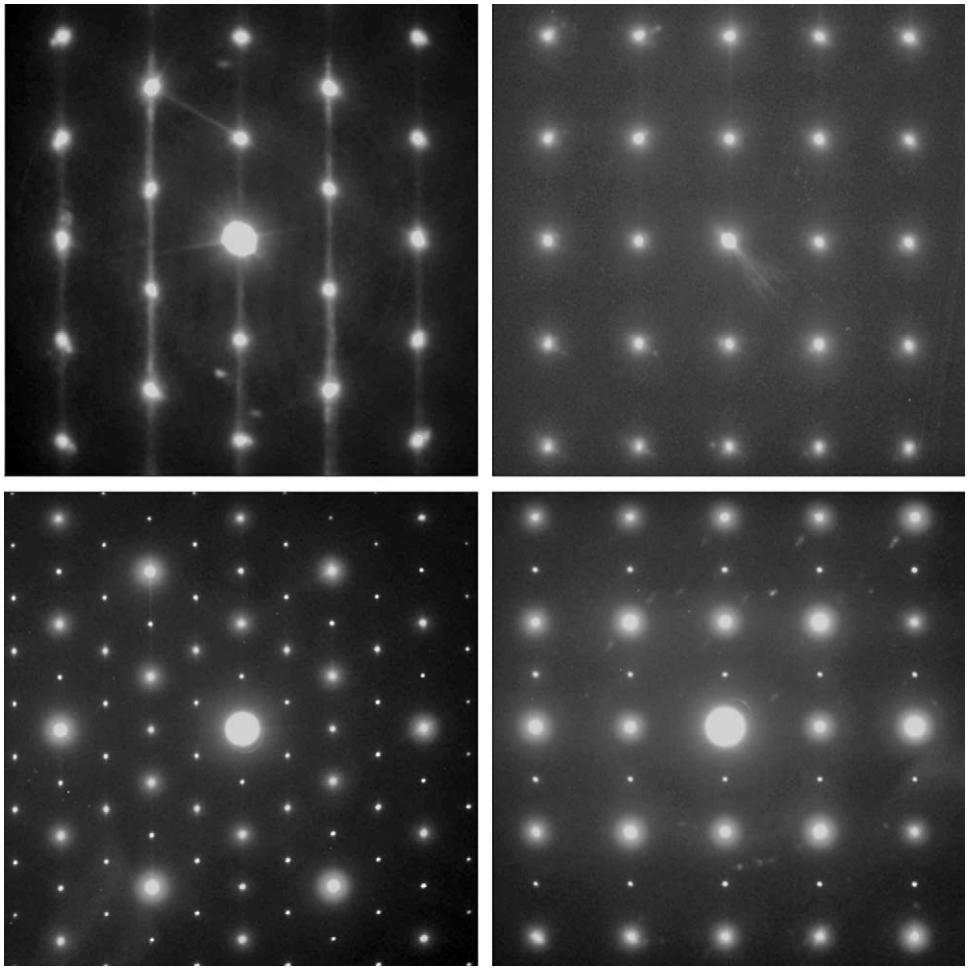

Fig. 1. Electron diffraction patterns along [0 0 1] (left) and [1 0 0] (right) axes for U_2PtSi_3 (upper) and U_2FeSi_3 (bottom).

4.073(7) Å and $c = 3.960(4)$ Å and no impurity phase can be detected.

For the comparison with U_2PtSi_3, the electron diffraction patterns of U_2FeSi_3 obtained along [0 0 1] and [1 0 0] axes are also presented in Fig. 1(bottom). In contrast to U_2PtSi_3, the patterns display a super spot, which indicates the doubling of the lattice parameter along *a*-axis. Also, the X-ray diffraction pattern shows a small reflection at 12.8° (see Fig. 2(b)). Among the distorted or ordered hexagonal/trigonal and orthorhombic/monoclinic derivatives of the AlB_2-type structure in the Bärnighausen tree [19], only the U_2RuSi_3-type structure (hexagonal, *P*6/*mmm*; see the inset Fig. 2(b)) can explain these results [20]. The small XRD peak at 12.8° is indexed as 1 0 0 peak of the U_2RuSi_3-type structure. The Rietveld analysis of the X-ray diffractions in the region of 10–90° reveals that the silicon atoms are on the 12*o* split positions (x, $2x$, 0.4433) with $x = 0.1750(15)$ and occupancy of 50% and the lattice parameters are $a = 8.003(10)$ Å and $c = 3.854(3)$ Å. We should mention that it is difficult to prepare a pure U_2FeSi_3 sample and some impurities were detected by the XRD measurements for our several polycrystalline and single crystalline samples in spite of the small weight loss of <0.2 wt.%. The Rietveld analysis of the XRD data (illustrated in Fig. 2(b)) suggests that three impurity phases, namely UFe_2Si_2 (tetragonal, *I*4/*mmm* [21], paramagnet [21], mass fraction ∼8%), $U_3Fe_2Si_7$ (orthorhombic, *Cmmm* [22], paramagnet [23], ∼2%) and UFeSi (orthorhombic, *Pnma* [24], paramagnet [25], ∼1%), seems to exist in the sample used in the present work.

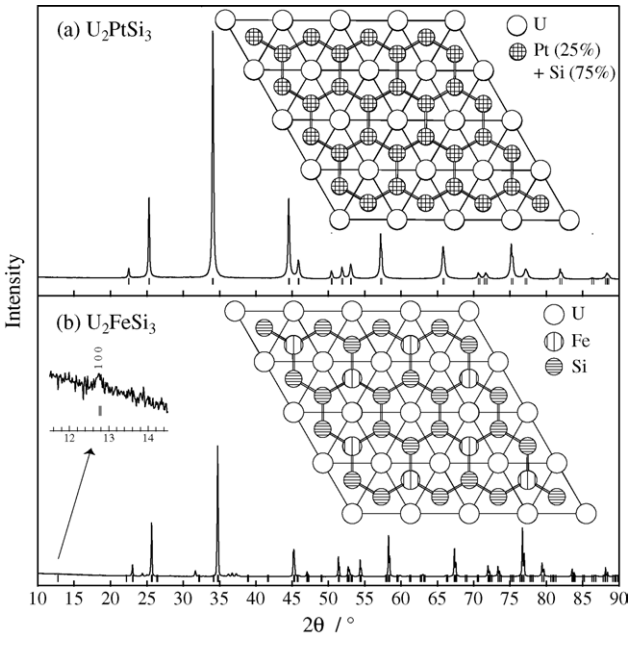

Fig. 2. X-ray diffraction patterns and calculated reflections indicated by small vertical bars for the phases of U_2PtSi_3 (a) and U_2FeSi_3 (b). Diffraction peak for (1 0 0) reflection of superstructure cell of U_2FeSi_3 is shown in inset (b). Crystal structure projected onto (0 0 1) plane for U_2PtSi_3 (a) and U_2FeSi_3 (b) (inset).

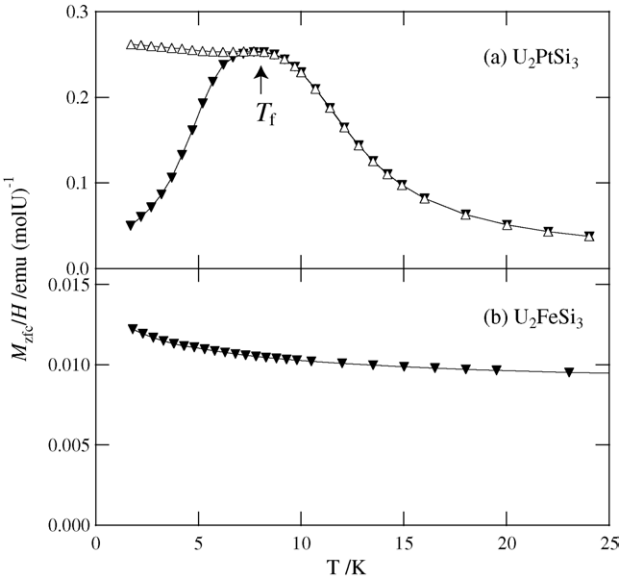

Fig. 3. (a) The temperature dependence of ZFC (closed triangle) and FC (open triangle) susceptibility (M/H) for U_2PtSi_3 in a magnetic field of 500 Oe [1] and (b) the temperature dependence of ZFC susceptibility for U_2FeSi_3 in a magnetic field of 500 Oe (1 emu $mol^{-1} = 4\pi \times 10^{-6}$ m^3 mol^{-1}).

3.2. Magnetic and electronic properties

The temperature variations of the zero-field-cooled (ZFC) magnetization M_{zfc} divided by the applied magnetic field H (hereafter called susceptibility) for U_2PtSi_3 and U_2FeSi_3 in the field of 500 Oe are compared in Fig. 3. For U_2PtSi_3 with random distribution of Pt and Si atoms in the AlB_2-type lattice, the M_{zfc}/H curve shows the typical feature of a spin glass material, i.e. an evident maximum at $T_f = 7.7$ K [1] and magnetic irreversibility manifests as the difference between the ZFC and field-cooled (FC) curves starting just below T_f. In contrast, for U_2FeSi_3 with ordered Fe and Si atoms in the U_2RuSi_3-type lattice, the M_{zfc}/H curve reveals the paramagnetic behavior down to 1.8 K with identical FC and ZFC curves. At high temperatures, the H/M_{zfc} data can be fitted well using the Curie–Weiss law for both U_2PtSi_3 and U_2FeSi_3.

Different magnetic behavior between U_2PtSi_3 and U_2FeSi_3 is also confirmed by the field dependence of magnetization measurements as shown in Fig. 4. At 5 K, evident hysteresis and remanence (with a value of 0.01 μ_B/U) are observed in $M(H)$ curve as usually observed in a spin glass. In contrast, $M(H)$ of U_2FeSi_3 is almost linear up to 1 T and no hysteresis and remanence is detected at 5 K.

In Fig. 5, we compare the temperature dependences of specific heat $C(T)$ and electrical resistivity $\rho(T)$ of U_2PtSi_3 and U_2FeSi_3. The formation of spin glass state in U_2PtSi_3 is further confirmed by a large γ value (obtained from the C/T versus T^2 plot at low temperatures, see the lower inset of Fig. 5(a)) and the absence of any anomaly at the temperature T_f (7.7 K), where the dc susceptibility shows a clear peak. The determined γ value of 198 mJ $(mol\ U)^{-1}$ K^{-2} is

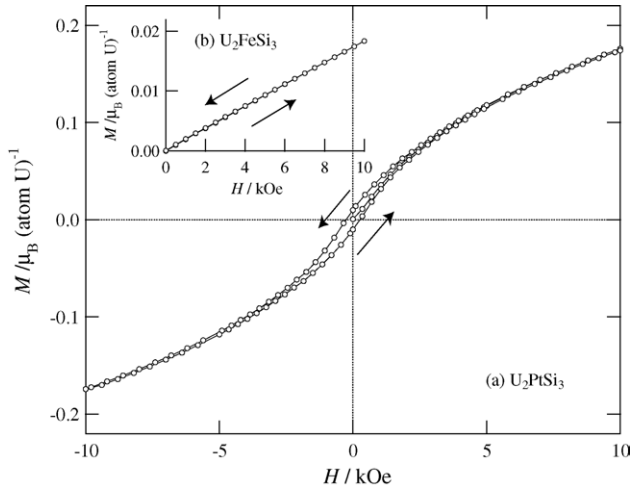

Fig. 4. Magnetization curves of (a) U_2PtSi_3 [1] and (b) U_2FeSi_3 (inset) at 5 K.

comparable to those obtained for other spin glass systems in the U_2XSi_3 family, such as U_2AuSi_3 [5] and U_2PdSi_3 [3]. Comparing with that, a relatively small γ value of 88 mJ (mol U)$^{-1}$ K^{-2} is determined for U_2FeSi_3 (see the lower inset of Fig. 5(b)), which agrees well with the literature value of 90 mJ (mol U)$^{-1}$ K^{-2} [9]. This value is also comparable to that obtained for the paramagnet U_2RuSi_3. On the other hand, the electrical resistivity also reveals the different behavior for U_2PtSi_3 and U_2FeSi_3. The former shows a relatively

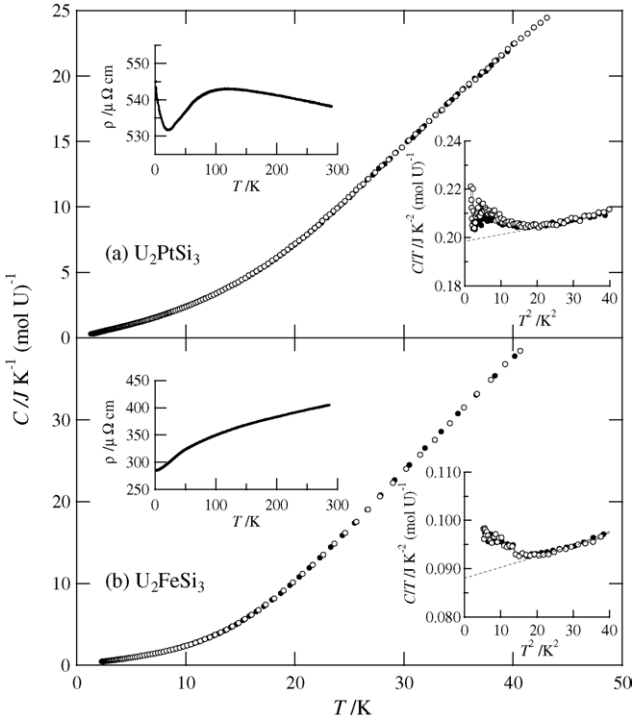

Fig. 5. Plots of C vs. T and plots of C/T vs. T^2 (upper inset) for U_2PtSi_3 [1] at 0 (closed circle) and 5 kOe (open circle) (a) and for U_2FeSi_3 at 0 (closed circle) and 50 kOe (open circle) (b), temperature dependences of resistivity for U_2PtSi_3 [3] (a, inset) and U_2FeSi_3 (b, inset).

large residual resistivity and the relatively weak temperature dependence over the temperature range measured, while a minimum in $\rho(T)$ appears at low temperatures (see the upper inset of Fig. 5(a)). In fact, we have observed the similar phenomena for U_2AuSi_3 and U_2PdSi_3, which can be attributed to the scattering due to structural disorder as is usually observed in metallic spin glasses. Note that such $\rho(T)$ behavior is not observed for the U_2RuSi_3-type compound U_2FeSi_3 (see the upper inset of Fig. 5(b)). These results are consistent with the above-mentioned crystallographic analysis for U_2PtSi_3 and U_2FeSi_3 based on our X-ray diffraction and electron diffraction, which show that the Pt and Si atoms in U_2PtSi_3 are statistically distributed on the B site of the AlB_2-type structure and the Fe and Si atoms in U_2FeSi_3 are ordered on the U_2RuSi_3-type lattice sites.

As mentioned in the introduction, both randomness and frustration of magnetic moments, i.e. competition between ferromagnetic and antiferromagnetic interaction, are necessary to form a spin glass [26]. The mechanism of spin glass behavior in the AlB_2-type compounds U_2AuSi_3, U_2PdSi_3, U_2PtSi_3 and U_2CuGa_3 can be understood as following [3]. Firstly, randomness could arise from the statistical distribution of the T and Si positions, which vary the electronic environment around the U atoms and seems to introduce a random U–U exchange interaction mediated by the 5*f*-ligand hybridization. Moreover, within one magnetic layer, U atoms form triangles of nearest neighbors. This geometrical arrangement of the U atoms is favorable to form frustrated magnetic moment. Obviously, the absence of spin glass features in the structurally ordered system U_2FeSi_3 can naturally be understood within this scenario. We should mention that the dynamic analyses of our ac susceptibility and magnetic relaxation measurements give further evidence for spin glass state in U_2PtSi_3 [1,3]. One could expect a much sharper peak in dc susceptibility of U_2PtSi_3 in lower fields.

It is interesting to note that Chevalier et al. [7] pointed out the existence of an orthorhombic superstructure with partial ordering arrangement of non-magnetic atoms in U_2RhSi_3. This intermediate distribution between the perfectly ordered U_2RuSi_3-type structure and the random AlB_2-type structure has not been confirmed for other member of the U_2XSi_3 family. Recently, we found that the electron diffraction pattern of U_2IrSi_3 reveals diffuse scattering, which is characteristic of such intermediate ordered structure. Note that instead of the simple spin glass behavior, the U_2IrSi_3 compound shows magnetic features characteristic of a cluster glass state [6] similar to that observed for U_2RhSi_3 [7]. This issue will be discussed in detail in the forthcoming paper.

4. Conclusion

Electron diffraction, X-ray powder diffraction and magnetization measurements were performed for the ternary uranium compounds U_2PtSi_3 and U_2FeSi_3. Comparing to the simple AlB_2-type structure in U_2PtSi_3, the electron

diffraction patterns of U_2FeSi_3 shows the superstructure doubling the lattice parameter as observed for U_2RuSi_3, suggesting the loss of random distribution of the non-magnetic atoms. These crystal structures are further confirmed by the XRD measurements. Moreover, different magnetic behaviors were also observed for U_2PtSi_3 and U_2FeSi_3. The non-magnetic atom disorder compound U_2PtSi_3 displays typical spin glass features at low temperature, in contrast, in the structurally ordered compound U_2FeSi_3, no spin glass behaviour is detected.

Acknowledgements

We would like to thank Mr. Y. Suzuki and Mr. M. Watanabe of the Irradiation Experimental Facility of Institute for Materials Research (IMR), Tohoku University and Professor I. Satoh and Mr. M. Takahashi of Experimental Facility for Alpha-Emitters of IMR, Tohoku University, for their kind cooperation. This work was performed at the Irradiation Experimental Facility, IMR, Tohoku University.

References

[1] D.X. Li, Y. Shiokawa, Y. Homma, A. Uesawa, T. Suzuki, J. Magn. Magn. Mater. 176 (1997) 261.
[2] A. Kimura, D.X. Li, Y. Shiokawa, Physica B 281–282 (2000) 247.
[3] D.X. Li, Y. Shiokawa, Y. Haga, E. Yamamoto, Y. Onuki, J. Phys. Soc. Jpn. 71 (2002) 418.
[4] D.X. Li, Y. Shiokawa, Y. Homma, A. Uesawa, T. Suzuki, Phys. Rev. B 57 (1998) 7434.
[5] D.X. Li, A. Kimura, Y. Homma, Y. Shiokawa, A. Uesawa, T. Suzuki, Solid. State Commun. 108 (1998) 863.
[6] D.X. Li, S. Nimori, Y. Shiokawa, Y. Haga, E. Yamamoto, Y. Onuki, Phys. Rev. B 68 (2003) 172405.
[7] B. Chevalier, R. Pöttgen, B. Darriet, P. Gravereau, J. Etourneau, J. Alloys Compd. 233 (1996) 150.
[8] D. Kaczorowski, H. Noël, J. Phys. Condens. Matter 5 (1993) 9185.
[9] N. Takeda, M. Ishikawa, J. Phys. Soc. Jpn. 67 (1998) 1062.
[10] V.H. Tran, J. Phys. Condens. Matter 8 (1996) 6267.
[11] V.H. Tran, F. Steglich, G. André, Phys. Rev. B 65 (2002) 134401.
[12] T. Yamamura, D.X. Li, Y. Shiokawa, Physica B 329–333 (2003) 559.
[13] V.H. Tran, R. Troc, D. Badurski, J. Alloys Compd. 199 (1993) 193.
[14] L. Shlyk, J. Stepien-Damm, J. Magn. Magn. Mater. 195 (1999) 37.
[15] F.G. Gandra, D.P. Rojas, L. Shlyk, L.P. Cardoso, A.N. Medina, J. Magn. Magn. Mater. 226–230 (2001) 1312.
[16] V.H. Tran, D. Daczorowski, T. Roisnel, R. Troc, H. Noël, F. Bourée, G. André, Physica B 205 (1995) 24.
[17] T. Yamamura, D.X. Li, K. Yubuta, Y. Shiokawa, J. Alloys Compd. 374 (2004) 226.
[18] F. Izumi, T. Ikeda, Mater. Sci. Forum 321–324 (2000) 198.
[19] R.-D. Hoffmann, R. Pöttgen, Z. Kristallogr. 216 (2001) 127.
[20] A diversity of derivatives related to AlB_2-type structure examined are hexagonal or trigonal derivatives of Er_2RhSi_3, NdPtSb, Ni_2In, YPtAs (No. 194), Ti_5Ga_4 (No. 193), Lu_2CoGa_3, Er_2RhSi_3 (No. 190), YbAgPb, SrPtSb, ScAuSi (No. 187), Pr_8CoGa_3, YLiSn (No. 186), $CeCd_2$, $EuGe_2$ (No. 164), CaLiSn (No. 156), and orthorhombic or monoclinic derivatives of $CeCu_2$, KHg_2 (No. 74), TiNiSi (No. 62), UPt_2 (No. 40), CaCuGe (No. 33), CaPtP (No. 26) [19].
[21] K.H.J. Buschow, D.B. De Mooij, Philips J. Res. 41 (1986) 55.
[22] L.G. Aksel'rud, Y.P. Yarmolyuk, I.V. Rozhdestvenskaya, E.I. Gladyshevskii, Sov. Phys. Crystallogr. 26 (1981) 103.
[23] F.G. Aliev, L.G. Aksel'rud, V.V. Kozyr'kov, V.V. Moshchalkov, Sov. Phys. Solid State 30 (1988) 742.
[24] A.V. Andreev, F. Honda, V. Sechovsky, M. Divis, N. Izmaylov, Cherna, J. Alloys Compd. 335 (2002) 91.
[25] F. Canepa, P. Manfrinetti, M. Pani, A. Palenzona, J. Alloys Compd. 234 (1996) 225.
[26] J.A. Mydosh, Spin Glasses: An Experimental Introduction, Taylor & Francis Ltd., London, 1993.